Membrane Decoration by Amphiphilic Block Copolymers in Bicontinuous Microemulsions

H. Endo,[1] J. Allgaier,[1] G. Gompper,[1] B. Jakobs,[2] M. Monkenbusch,[1] D. Richter,[1] T. Sottmann,[2] and R. Strey[2]

[1]*Institut für Festkörperforschung, Forschungszentrum Jülich, D-52425 Jülich, Germany*

[2]*Institut für Physikalische Chemie, Universität zu Köln, Luxemburger Strasse 116, D-50939 Köln, Germany*

(Received 17 February 2000)

The effect of various amphiphilic block copolymers of different molar masses on the structure and phase behavior of ternary amphiphilic systems (water, oil, and nonionic surfactant) is investigated. Small amounts of PEP-PEO block copolymer lead to a dramatic increase in the volumes of oil and water, which can be solubilized in a bicontinuous microemulsion. High-precision neutron scattering experiments with a sophisticated contrast variation technique demonstrate that the polymers form uniformly distributed mushroom conformations on the surfactant membrane. Based on these observations, we propose a universal mechanism for the swelling behavior, which is due to the variation of the membrane curvature elasticity.

PACS numbers: 61.25.Hq, 61.12.Ex, 82.70.–y

The effect of polymers on the behavior of amphiphilic bilayers in water has received much attention recently. Water-soluble polymers and polymer networks, which are attached to lipid bilayers, are very common in all kinds of biological membranes. Polymers anchored to phospholipid bilayers have also been used to protect artificial vesicles against the body's immune response, and thereby make "stealth liposomes" effective drug carrier systems [1]. The increased lifetime of stealth liposomes has been attributed to a *steric repulsion* which arises from the reduced polymer entropy when the polymer layer is compressed, as it is well known in the steric stabilization of colloidal systems against coagulation [2].

The polymer decoration of membranes is expected theoretically to increase the *bending rigidity* [3–5]. This effect has been observed qualitatively in micropipet aspiration experiments of vesicles with PEO lipids *above* the overlap concentration [6], and for lamellar phases of membranes with hydrophilic polymers with hydrophobic side chains below the overlap concentration [7]. In both cases, the bending rigidity was found to increase, but then to level off with increasing polymer concentration. On the other hand, the bending rigidity was found to vary very little with the polymer concentration both in the lamellar phase in Ref. [8] and in surfactant bilayer vesicles with PEO surfactants [9]. A quantitative comparison with theory has therefore not been possible so far.

We want to investigate in this paper the effect of a nearly symmetric amphiphilic block copolymer (D) on the structure and phase behavior of ternary amphiphilic system of water (A), oil (B), and surfactant (C). The addition of polymer in small amounts has been found to lead to a dramatic decrease in the surfactant concentration, which is needed to solubilize oil and water [10]. We will show below by a detailed analysis of high-precision neutron scattering data and a theoretical calculation of the phase diagram that the block copolymers are incorporated into the surfactant layer where they form mushroom conformations. Thereby they modify the elastic moduli of the layer such that the formation of passages between neighboring membranes is hindered.

We consider microemulsions consisting of equal amounts of water and n-decance, the nonionic surfactant $C_{10}E_4$ (n-decyl-tetraoxyethylene), and small amounts of the amphiphilic block copolymers PEPx-PEOy (polyethylenepropylene-*co*-polyethyleneoxide), where x and y denote the molecular weights of each block in kg/mol. The polymers were synthesized by living anionic polymerization and show a narrow molecular weight distribution [11]. The chemical structure of the polymers mimics the structure of the C_iE_j surfactant, and PEP10-PEO10 corresponds roughly to $C_{715}E_{230}$.

For nonionic microemulsions temperature induces phase inversion by changing the spontaneous curvature of the surfactant film [12]. The lower-phase o/w microemulsion ($\underline{2}$) inverts to a w/o microemulsion ($\bar{2}$) with increasing temperature; see Fig. 1. At intermediate temperatures, the microemulsion coexists with water- and oil-excess phases, while at sufficiently high volume fractions ϕ_C of the surfactant a one-phase region is found. The temperature-composition diagram of the ternary system has the characteristic shape of a fish, the three-phase region forming the fish body and the adjacent one-phase region the fish tail. The point of optimal solubility in the fish tail is located at the lower ϕ_C the more efficient the surfactant. Addition of an amphiphilic PEPx-PEOy polymer increases the efficiency of the mixture dramatically. This effect becomes stronger with increasing volume fraction δ_V of block copolymer in the mixture of both amphiphiles. It is important to note that at the same time the phase inversion temperature of the microemulsion remains constant (for symmetric PEPx-PEOy) or shifts only marginally (for asymmetric PEPx-PEOy) [10].

Small angle neutron scattering (SANS) experiments were performed on samples in the bicontinuous phase close to the optimal point ($\phi_C = 0.05$), which contain $\delta_V = 0.1$ of the amphiphilic PEP5-PEO15 block copolymer. With neutrons as probe, contrast variation techniques

 0031-9007/00/85(1)/102(4)$15.00

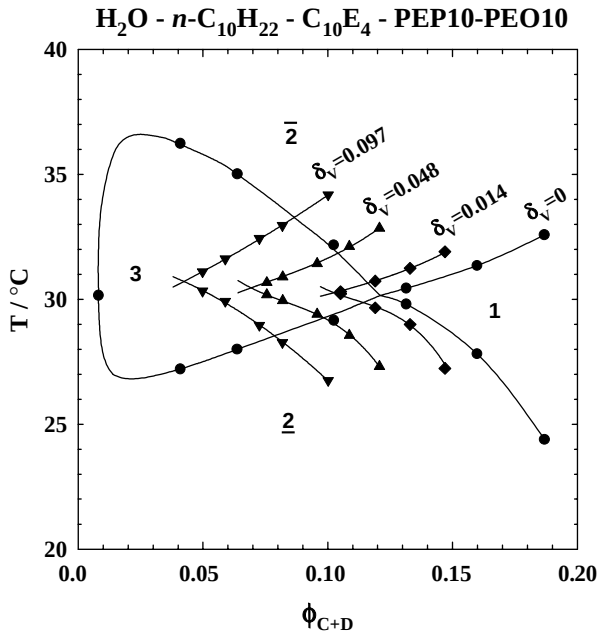

FIG. 1. Three-phase body (3) and adjacent one-phase (1) region for water-*n*-decane-$C_{10}E_4$. Addition of the amphiphilic block copolymer PEP10-PEO10 shifts the one-phase region to smaller amphiphile volume fraction ϕ_{C+D}. $\underline{2}$ and $\bar{2}$ refer to o/w and w/o microemulsions in equilibrium with their respective excess phases.

based on H/D replacement can be used to modify the visibility of different components in the system.

In bulk contrast, with deuterated water and protonated oil, the scattering is dominated by the three-dimensional structure of the water network; any film or polymer contributions are only marginal. In principle, the location and structure of the polymer in the bicontinuous microemulsion can be examined in a system where all components except the polymer have exactly the same scattering length densities ρ_i [with $i = w, o, f, p$ for water, oil, film (or surfactant), and polymer, respectively]; i.e., deuterated and protonated constituents have to be mixed such that $\rho_w = \rho_o = \rho_f \neq \rho_p$. However, since the thus obtained polymer scattering is about 5 orders of magnitude lower than the bulk contrast and 2 orders of magnitude lower than film-contrast scattering (only surfactant protonated) the required perfect match of the scattering length densities of water, oil, *and* surfactant is practically unfeasible. On the other hand, a careful analysis of data obtained close to the matching point yields (among others) the required polymer scattering functions. The scattering intensity, $I(Q)$, after background subtraction is given by

$$I(Q) = \sum_{i,j=\{o,f,p\}} (\rho_i - \rho_w)(\rho_j - \rho_w) S_{i,j}(Q), \qquad (1)$$

where $S_{i,j} = \int \langle c_i(\vec{r}_i) c_j(\vec{r}_j) \rangle \exp[i\vec{Q} \cdot (\vec{r}_i - \vec{r}_j)]\, d^3\vec{r}$. Here, $c_i(\vec{r})$ describes the volume fraction of component i at position $\vec{r}$, and ρ_i is the scattering length density. In Eq. (1), water is arbitrarily chosen as the component of the system that is considered as background.

In the experiment performed on the high intensity SANS instrument D22 at the ILL in Grenoble, contrast variation around the two-dimensional matching point was achieved by a stepwise increment of ρ_o (adding tiny amounts of protonated decane) and ρ_f (adding protonated surfactant), which produced 15 different samples covering the ranges $\rho_o \in [6.3, 6.54] \times 10^{10}$ cm^{-2} and $\rho_f \in [5.91, 6.88] \times 10^{10}$ cm^{-2}. Their scattering data were then used to extract the six partial scattering functions $S_{o,o}$, $S_{f,f}$, $S_{o,f}$, $S_{o,p}$, $S_{f,p}$, and $S_{p,p}$ by inserting the measured intensities $I_m(Q)$ and the contrasts $(\rho_i^m - \rho_w)$ into Eq. (1) and solving the overdetermined set of equations ($m = 1, \ldots, 15$) by singular value decomposition separately for each Q value. We can improve the reliability of the results by adding pure bulk- and film-contrast data with very large weight as well as the relation $S_{o,f} = -(1/2)S_{f,f}$ derived in Ref. [13] to this set of equations. The exact matching point could then be refined by reconstructing the $I_m(Q)$ values from the obtained partial structure factors $S_{i,j}$ and minimizing the deviations from the experiment data. Investigation of the sensitivity of the $S_{i,j}$ on the exact location of the matching point revealed only that $S_{o,p}$ is so sensitive that no reliable form can be inferred.

Figure 2a shows the result for the polymer, $S_{p,p}$, and film, $S_{f,f}$, scattering functions. The comparison of the

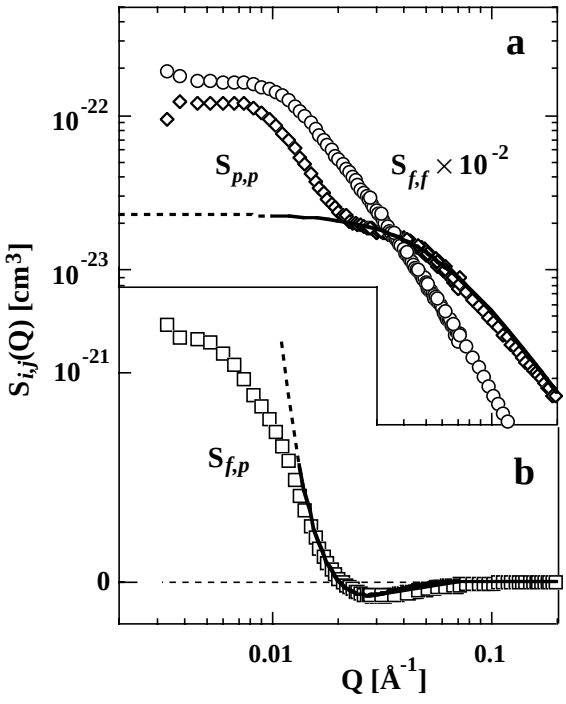

FIG. 2. Experimental partial scattering functions. (a) $S_{p,p}$ (◇), in comparison with $S_{f,f}$ (○) and calculated polymer coil scattering (solid line); see text. (b) $S_{f,p}$ (□), which contains the interference between surfactant film and extended polymer layer, and fit to the calculated intensity (solid line) for ideal chains anchored to a planar membrane; see text. Note the linear scale of the ordinate.

scattering curves indicates that the polymer scattering $S_{p,p}$ follows the form of $S_{f,f}$ for small $Q < 0.02$ Å^{-1}. This demonstrates clearly that the polymer "decorates" the surfactant film. Because of the dilution of scattering length density, however, the corresponding intensity is about 2 orders of magnitude lower than the pure film-contrast scattering. For wave vectors $Q > 0.03$ Å^{-1}, on the other hand, $S_{p,p}$ reflects the scattering from the polymer coils. The solid line in Fig. 2a shows a fit to the Zimm formula [14], which contains the Debye function and includes the effect of the second virial coefficient to account for the interchain interactions in the interface. Any polymer-polymer aggregation (micellization) would immediately lead to orders of magnitude higher values for $S_{p,p}$ [11] and can be safely excluded. The film-polymer scattering, $S_{f,p}$, shown in Fig. 2b, exhibits a minimum at $Q \simeq 0.03$ Å^{-1}, which is mainly due to maxima in the polymer density at a distance $\beta\mathcal{R}_{\mathrm{PEP}}$ and $\beta\mathcal{R}_{\mathrm{PEO}}$ from the interface, where $\mathcal{R}$ is the average end-to-end distance of a polymer coil, and $\beta = 4\ln 2/(3\sqrt{6}) = 0.38$ for ideal chains [15]. The solid line is a fit of the Fourier transform of the monomer density projected on the film-surface normal, as expected theoretically for ideal chains in the mushroom regime [15], including a Q^{-2} factor to account for the angular averaging (valid only for $Q > 0.01$ Å^{-1}). The fitted average end-to-end radius amounts to 155 Å, which compares quite well with the end-to-end distance $\mathcal{R}_{\mathrm{PEO}} = 140$ Å determined from homopolymer solutions [16]; it is much smaller than the average domain size of 550 Å.

The experimental results prove that the polymer is tethered to the interface, and that the "mushrooms" formed by the PEP chain in the oil phase and by the PEO chain in water are *not* noticeably influenced by the presence of neighboring membranes.

The structure and phase behavior of microemulsions has been modeled very successfully as an ensemble of thermally fluctuating membranes [17–22] in recent years. The shape and fluctuations of *homogeneous* membranes are controlled by the curvature energy [23]

$$\mathcal{H}_b = \int dS \left[\frac{\kappa}{2} (c_1 + c_2 - 2c_0)^2 + \bar{\kappa} c_1 c_2 \right], \quad (2)$$

where c_1 and c_2 are the principal curvatures at each point of the membrane, c_0 is the spontaneous curvature, and κ and $\bar{\kappa}$ are the bending rigidity and saddle-splay modulus, respectively.

The effect of a polymer decoration on membrane elasticity has already been calculated in Refs. [3–5] for ideal chains (without self-avoidance). For a number density, σ, of block copolymer within the membrane, the results can be written in the universal scaling form

$$\kappa_{\mathrm{eff}} = \kappa + \frac{k_B T}{12} \left(1 + \frac{\pi}{2}\right) \sigma(\mathcal{R}_w^2 + \mathcal{R}_o^2), \quad (3)$$

$$\bar{\kappa}_{\mathrm{eff}} = \bar{\kappa} - \frac{k_B T}{6} \sigma(\mathcal{R}_w^2 + \mathcal{R}_o^2), \quad (4)$$

where $\mathcal{R}_{w/o}$ is the end-to-end distance of hydrophilic/hydrophobic polymer block. It is important to note that these results are obtained from a superposition of the effects of independent chains under the assumption that the curvature is distributed *uniformly* over the whole surface. Strictly speaking, this is correct only when the mushrooms just begin to overlap. For smaller concentrations, the membrane is inhomogeneous. It is well known that two-component membranes with inhomogeneous *spontaneous* curvature (but homogeneous bending rigidity) actually have a *lower* effective rigidity [24] than the pure membranes of each component. However, in our case of small or vanishing spontaneous curvature, we can expect Eqs. (3) and (4) to be good approximations also below the overlap concentration $\sigma^* = 1/\max(\mathcal{R}_o^2, \mathcal{R}_w^2)$. Also, a local deformation of the membrane near the anchoring points of the polymers [25] should not occur.

In the case of vanishing spontaneous curvature, the phase behavior of the curvature model (2) is controlled by κ, $\bar{\kappa}$, and the membrane volume fraction ψ. In particular, it has been argued [19,20] that the lamellar phase can be stable only with respect to a proliferation of topological defects, which are passages between neighboring oil or water layer, for ψ larger than

$$\ln(\psi/\psi^*) = \frac{2\pi}{\alpha_-} \bar{\kappa}/k_B T, \quad (5)$$

where $\alpha_- = 5/3$ and ψ^* is a constant of order unity. The form of the instability, Eq. (5), arises from the effect of thermal short wavelength fluctuations on the rigidities κ and $\bar{\kappa}$ on larger length scales [26]. Monte Carlo simulations of randomly triangulated surfaces [21] nicely confirm this picture; furthermore, the simulations show that at constant κ the microemulsion coexists with excess oil and water phases along a line, which runs almost parallel to the instability line, Eq. (5). By inserting $\bar{\kappa}_{\mathrm{eff}}$, Eq. (4), for $\bar{\kappa}$ in Eq. (5), we arrive at the expression

$$\ln(\psi) = \ln(\psi_0) - \Xi\sigma(\mathcal{R}_w^2 + \mathcal{R}_o^2) \quad (6)$$

with

$$\Xi = \frac{\pi}{5} = 0.628\ldots \quad (7)$$

for the dependence of the membrane volume fraction ψ of the microemulsion at the optimal point on the polymer concentration, where ψ_0 is the optimal membrane volume fraction of the pure system.

A test of this prediction can be made by inserting the experimental values of the end-to-end distances $\mathcal{R}_w$ and $\mathcal{R}_o$ into Eq. (6) and plotting $\ln(\psi)$, as a function of the scaled area of the membrane per polymer chain. The result is shown in Fig. 3. The data for PEP-PEO block copolymers with four different chain lengths nicely fall onto a single straight line in this plot, which confirms the scaling form of Eq. (6), and which provides strong evidence that the main

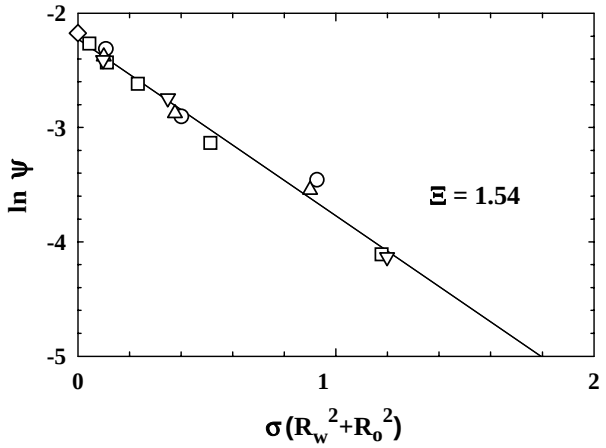

FIG. 3. Membrane volume fraction ψ at the optimal point vs scaled polymer area $\sigma(R_w^2 + R_o^2)$. Pure system (◇), PEP5-PEO5 (▽), PEP10-PEO10 (△), PEP22-PEO22 (□), and PEP5-PEO15 (○).

effect of the polymer is indeed to modify the saddle-splay modulus of the membrane. The slope is found to be

$$\Xi = 1.54 \pm 0.05\,, \tag{8}$$

roughly twice as large as the theoretical estimate (7) for ideal chains. This indicates that self-avoiding chains have a considerably more pronounced effect on the curvature elastic moduli than ideal chains.

Figure 3 also shows that the largest polymer concentrations are already quite close to the overlap concentration, which is located at $\sigma(\mathcal{R}_w^2 + \mathcal{R}_o^2)$ between 1 and 2 (where the limiting cases correspond to strongly asymmetric and symmetric block copolymers, respectively). At this point, Eqs. (3) and (4) cease to be valid, because the brush regime is entered [3].

Our results demonstrate very clearly that the effect of anchored polymers on the behavior of a membrane ensemble is quite universal, and depends only on the dimensionless quantity $\sigma(\mathcal{R}_w^2 + \mathcal{R}_o^2)$. Therefore, in the case of good solvents examined here, the chemical structure enters only via the end-to-end distances of its polymer coils. The swelling upon polymer addition should occur in a very similar way also in sponge phases of amphiphilic bilayers, as they are encountered in the system of Ref. [7]. Furthermore, a similar swelling should occur in the lamellar phase. Such an effect is indeed visible in the data of Ref. [8], but has not been analyzed or discussed in any detail so far.

Polymers anchored to membranes provide a convenient handle to control the saddle-splay modulus, and thereby the preference of a membrane to form sponge, lamellar, or vesicle structures. A particularly interesting way of changing the elastic moduli would be to add homopolymers to the mixture, or to change the solvent quality by changing pH or mixing different fluids. An extreme case would be a theta solvent, where the polymers begin to collapse into a compact state.

Helpful discussions with E. Eisenriegler about polymers near surfaces are gratefully acknowledged.

[1] D. D. Lasic, *Liposomes: From Physics to Applications* (Elsevier, New York, 1993).
[2] S. T. Milner, Science **251**, 905 (1991).
[3] C. Hiergeist and R. Lipowsky, J. Phys. II (France) **6**, 1465 (1996).
[4] E. Eisenriegler, A. Hanke, and S. Dietrich, Phys. Rev. E **54**, 1134 (1996).
[5] C. M. Marques and J. Fournier, Europhys. Lett. **35**, 361 (1996).
[6] E. A. Evans and W. Rawicz, Phys. Rev. Lett. **79**, 2379 (1997).
[7] Y. Yang *et al.*, Phys. Rev. Lett. **80**, 2729 (1998).
[8] H. E. Warriner *et al.*, Science **271**, 969 (1996); Biophys. J. **75**, 272 (1998).
[9] R. Joannic, L. Auvray, and D. D. Lasic, Phys. Rev. Lett. **78**, 3402 (1997).
[10] B. Jakobs *et al.*, Langmuir **15**, 6707 (1999).
[11] J. Allgaier, A. Poppe, L. Willner, and D. Richter, Macromolecules **30**, 1582 (1997); A. Poppe *et al.*, Macromolecules **30**, 7462 (1997).
[12] R. Strey, Curr. Opin. Colloid Interface Sci. **1**, 402 (1996).
[13] G. Gompper and M. Schick, Phys. Rev. B **41**, 9148 (1990).
[14] J. S. Higgins and H. C. Benoit, *Polymers and Neutron Scattering* (Clarendon Press, Oxford, 1994).
[15] E. Eisenriegler, K. Kremer, and K. Binder, J. Chem. Phys. **77**, 6296 (1982).
[16] S. Kawaguchi *et al.*, Polymer **38**, 2885 (1995).
[17] G. Gompper and M. Schick, in *Phase Transitions and Critical Phenomena*, edited by C. Domb and J. Lebowitz (Academic Press, London, 1994), Vol. 16, pp. 1–176.
[18] D. C. Morse, Curr. Opin. Colloid Interface Sci. **2**, 365 (1997).
[19] L. Golubović, Phys. Rev. E **50**, R2419 (1994).
[20] D. C. Morse, Phys. Rev. E **50**, R2423 (1994).
[21] G. Gompper and D. M. Kroll, Phys. Rev. Lett. **81**, 2284 (1998).
[22] T. Tlusty, S. A. Safran, R. Menes, and R. Strey, Phys. Rev. Lett. **78**, 2616 (1997).
[23] W. Helfrich, Z. Naturforsch. **28c**, 693 (1973).
[24] S. Leibler and D. Andelman, J. Phys. (Paris) **48**, 2013 (1987); M. M. Kozlov and W. Helfrich, Langmuir **8**, 2792 (1992).
[25] R. Lipowsky, Europhys. Lett. **30**, 197 (1995).
[26] F. David, in *Statistical Mechanics of Membranes and Surfaces*, edited by D. Nelson, T. Piran, and S. Weinberg (World Scientific, Singapore, 1989), pp. 157–223.